Article ID: 1000-324X(2012)01-0102-05 **DOI:** 10.3724/SP.J.1077.2011.11325

Preparation of 3D Ceramic Meshes by Direct-write Method and Modulation of Its Photocatalytic Properties by Structure Design

CAI Kun-Peng[1], LI Ya-Yun[1], SUN Zhen-Xin[1], SUN Jing-Bo[1], LI Bo[1,2], Zhou JI[1]

(1. State Key Laboratory of New Ceramics and Fine Processing, Department of Materials Science and Engineering, Tsinghua University, Beijing 100084, China; 2. Advanced Materials Institute, Graduate School at Shenzhen, Tsinghua University, Shenzhen 518055, China)

Abstract: 3D meshes of TiO_2 were fabricated by direct writing and subsequently sintered at 1150℃ for 2 h in an air atmosphere for photocatalytic degradation (PCD) of methylene blue(MB) solution. The crystal structure and morphology of the samples were determined by X-ray diffraction(XRD) and scanning electron microscope(SEM). PCD properties of the sintered meshes were obtained in an ultraviolet-visible light spectrophotometer, and were found to be better than that of cylindrical samples with the same weight. Three kinds of mesh structures were designed, sintered and measured. The results show that reasonable design could cause significant enhancement in the PCD activity by more than 60%. This enhancement could be attributed to irradiation absorption increment, which was caused by structure design of photocatalyst.

Key words: direct-write; ceramics; photocatalysis; TiO_2

Recently, TiO_2 photocatalysis has attracted constant research on treatment of polluted water[1], due to its good photo-stability, chemically and biologically inert nature and low cost[2]. The photocatalytic degeneration (PCD) reaction mechanism and kinetics have been reported to be modulated by surface modifications of photocatalyst, such as sensitization[3-4], platinization[5], charge modification[6], and fluorination[7-8]. Surface modifications have received great attention, while there are few reports on structure design of photocatalyst. With the ability of forming arbitrarily designed 3D structures, direct writing technique is one of the promising approaches to pattern materials at micro- and mesoscale[9-10]. Structures assembled by direct writing are formed with extruded ink rods in a layer by layer way, and could be utilized in ceramics structure construction[11-12], tissue engineering scaffolds[13], electromagnetic bandgap crystals[14-15] and flexible electronics[16-17]. It is possible, interesting and meaningful to combine this technique with PCD reactions.

In present work, we have developed a water based TiO_2 colloidal ink and constructed three designs of meshes by direct writing. Then the PCD properties of sintered meshes in methylene blue (MB) solution were studied. Results showed that reasonable design of mesh structure will cause significant enhancement in the activity of photocatalyst.

1 Experimental

1.1 Preparation of colloidal inks

Commercial TiO_2 nanoparticle powders (primary particle diameter, d=21 nm, specific surface area of 50 m^2/g; Aeroxide® TiO_2 P25) were added into water part by part. At the same time ultrasonication was used to reduce agglomerates. The mixture was then homogenized through continuous stirring to obtain inks suitable for extrusion. Inks with solid content of 42.5wt% were finally prepared for following studies.

1.2 Direct write assembly of 3D meshes

The 3D mesh was created layer by layer on a computer controlled robotic stage (A3200, Aerotech Inc., Pittsburgh, PA). A 2D in-plane pattern layer was firstly created by deposition of ink rods through nozzle attached to a syringe pump. The axes of the rods are parallel to each other with a pitch of constant value. After one layer was accomplished, an upper perpendicular layer was then deposited on the first one. Procedure would be continued until the designed structure was wholly built. The final assembled mesh structures were dried at 50℃ for 24 h and then sintered at 1150℃ for 2 h in air. Three kinds of meshes with the same cross section area, weight and layer number were

Received date: 2011-06-02; **Modified date:** 2011-08-24; **Published online:** 2011-10-09
Foundation item: National Natural Science Foundation of China (90922025, 50632030, 50921061, 10774087, 51032003)
Biography: CAI Kun-Peng(1987–), male, candidate of PhD. E-mail: ckp08@mails.tsinghua.edu.cn
Corresponding author: LI Bo, associate professor. E-mail: boli@mail.tsinghua.edu.cn

designed and created by controlling computer program. Commercial pre-sintered TiO_2 powders of the same weight with the sintered meshes were pressed uniaxially under a pressure of 10 MPa to make common cylindrical green compacts. The samples were all then sintered at 1150℃ for 2 h in air for comparison experiments. The sintered mesh structure has a tetragonal shape, with a 6.08 mm× 6.08 mm square top surface and height of 2.68 mm, while the sintered cylindrical compact has a top diameter of 7.94 mm and height of 1 mm.

1.3 Characterization of structure, phase and PCD properties

MB solution with concentration of 2 mg/L was prepared for PCD properties test of photocatalyst. The test was accomplished by following two steps: the irradiation step and the measuring step. In the irradiation step, 1.5 mL MB solution received ultraviolet (UV) irradiation from UV curing light source (with a main emission peak at 365 nm, Cure Spot^{TM} 50, ADAC Systems^{TM}, Torrington) for a set long time in the absence or presence of TiO_2 meshes. In the measuring step, the meshes were taken out. Then the transmittance and absorbance spectra of the MB solution were recorded through a UV-visible light spectrophotometer (Unicam UV 500, Thermo spectronic, England).

X-ray diffraction pattern of sintered sample was obtained using diffractometer (XRD-7000, Shimadzu, Japan). Surface morphology of meshes was scanned using micro-computed tomography (Axio Imager.Z1m, Carl Zeiss Shanghai Co. Ltd., China) and scanning electronic microscope (SSX-550, Shimadzu, Japan).

2 Results and Discussion

The as-dried mesh structure is shown in Fig. 1(a), while the cross section is shown in Fig. 1(b). Mesh with rod diameter of 230 μm and inter-rod distance (in-plane center-to-center rod spacing) of 400μm was obtained. Figure 1(c) shows the surface morphology of sintered mesh. A surface with dense grains is well developed, which means that the mesh have formed ceramics after being sintered. The main content of the prepared samples is rutile phase according to the XRD pattern of sintered ceramic powders shown in Fig. 1(d). As TiO_2 rutile crystal is photocatalytic[18-19], the present work is focused on the structure design of photocatalyst.

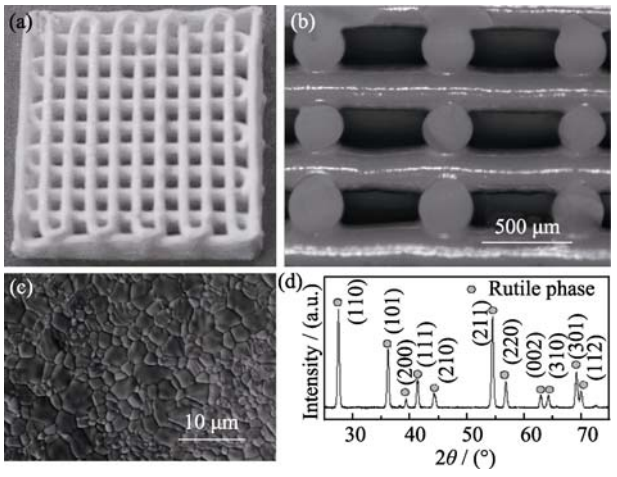

Fig. 1　(a) Optical graph of as-dried mesh; (b) Image of cross section of sintered mesh; (c) SEM image of mesh surface; (d) XRD pattern of sintered sample

The top, front and side view of a typical mesh structure is shown in the left side of Fig. 2(a). Mesh sample was placed carefully in quartz sampling cell to make the top plane face the irradiation direction, as shown in Fig. 2(a). For blank experiment, the transmittance spectra of the MB solution with no photocatalyst was tested with the irradiation time of 0 s, 90 s, 180 s, 270 s, 360 s and 450 s, respectively. The transmittance of MB solution increased slightly with irradiation time, as shown in Fig. 2(b). It is indicated that MB solution shows little trend to bleach when being exposed to UV irradiation in the absence of TiO_2 photo-catalyst. Figure 2(c) showed the transmittance spectra of the MB solution irradiated in the presence of TiO_2 mesh and cylindrical sample, and the irradiation time was 270 s. Two characteristic features were found: 1) the presence of TiO_2 photocatalyst could greatly improve the transmittance of after-irradiated the MB solution; 2) the PCD activity of mesh structure was better than that of the cylindrical sample, as solution catalyzed by cylindrical sample with larger irradiated surface area showed lower transmit tance after irradiation of the same time. Hence,

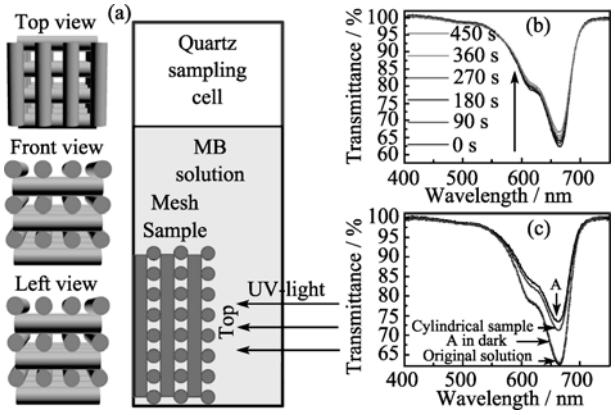

Fig. 2　(a) Schematic diagram of the irradiation step, (b) the transmittance of the MB solution with none photocatalyst after irradiation of 0 s, 90 s, 180 s, 270 s, 360 s and 450 s, and (c) the transmittance of the MB solutions catalyzed by cylindrical sample and mesh structure A for 270 s, dark environment experimental results of mesh structure A for 270 s are also provided. Left inset in (a) shows the top view, front view and left view of a typical mesh structure

three aspects are crucial to modulate the PCD reaction of the MB solution: the presence and choice of photocatalyst, time of the reaction and the inner space structure of photocatalyst. In addition, little difference was found in the transmittance of the MB solution in dark environment experiments using mesh structure A after 270 s without UV irradiation, as shown in Fig. 2(c). This indicates that absorption of the MB on the photocatalyst surface can be reasonably neglected for the sintered samples.

Here we propose three designs of layer-by-layer mesh structure, named A, B and C, respectively, as shown in Fig. 3. The rod directions of adjacent layers are perpendicular to each other (Fig. 3(a)-(c)). As for structure A, the rod arrangements are same to each other in both odd and even layers(Figs. 3(d), (g)). For structure B, there is an in-plane transverse displacement of 1/2 the inter-rod distance in two adjacent odd layers(Fig. 3(e)), while the rod arrangements are same to each other in even layers(Fig. 3(h)). Structure C was achieved by shifting alternative odd and even layers by 1/2 the inter-rod distance (Figs. 3(f), (i)). The three designed structures have the same weight and height, as well as the top area. The above mentioned three kind of meshes were assembled and sintered for the following experiments. Meanwhile, the four sides of meshes were blocked off, so that all the data was for illumination down the [001] axis of the log-pile.

The transmittance results was obtained in the measurement step for structure A, B and C, as illustrated in Fig. 4(a). For each structure design, the value of transmittance increased with irradiation time. For MB solutions, which received irradiation of the same time, the transmittance increased obviously from structure A to C. So the bleaching of MB solution could be enhanced by prolonging irradiation time and changing photocatalyst structure. Furthermore, the transmittance of MB solution in the presence of structure A for irradiation of 450 s was found to be approximately equal to that of structure C for irradiation of 270 s, as shown in Fig. 4(b). This means that the efficiency of photocatalyst could be improved greatly by replacing structure A with structure C.

This enhancement in the degeneration of MB solution could be explained considering increment in irradiation absorption, which was caused by structure design. There are displacements of 1/2 the inter-rod distance in both adjacent odd and even layers in structure C and no displacement in structure A, while structure B is a one-axis staggered log-pile. The capability to reflect and scatter incident light was strengthened from A to C because of increase in the effective cross section area, when there was a illumination down the [001] axis, where A has open channels while C does not. Hence, more reflecting and scattering of light took place in the inner space of structure C than A. As a result, more irradiation was absorbed by both photocatalyst and MB solution and more MB solution was degenerated. So the transmittance of MB solution photocatalysed by structure C was higher than that of structure A, with transmittance of structure B in the middle.

To confirm the relationship between PCD of MB solution and irradiation absorption, a brief inspection of the

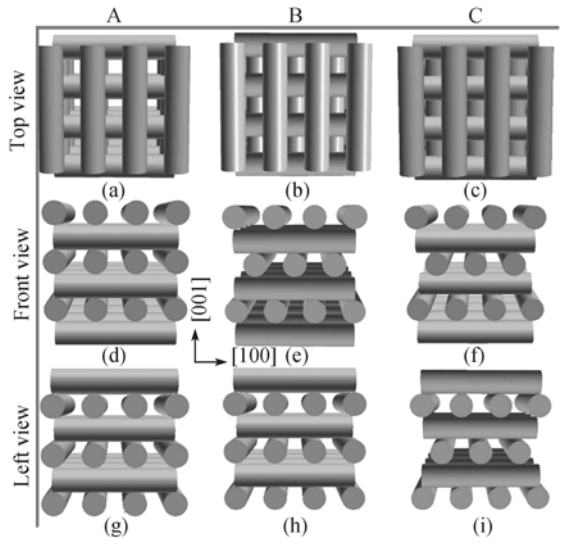

Fig. 3 Schematic illustrations of three mesh designs: top view of (a) A, (b) B, (c) C, front view of (d) A, (e) B, (f) C, and left view of (g) A, (h) B, (i) C

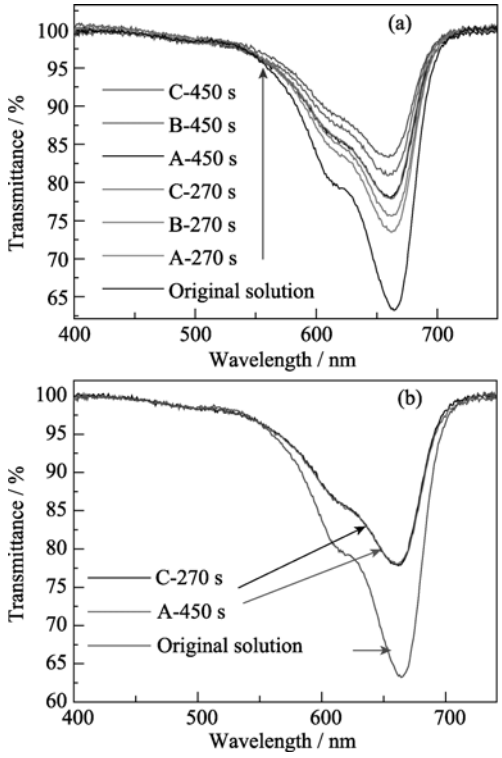

Fig. 4 Transmittance spectra of MB solution catalyzed by (a) structure A, B and C for 270 s and 450 s, (b) structure A for 450 s and structure C for 270 s

UV-visible absorption spectra of pure water was taken. Figure 5(a) shows the UV-visible absorption spectrum obtained from water of 1.5 mL, with mesh placed in. When no mesh was placed in water, there was no absorption of light. However, the absorbance of MB solution reached certain high value, when the mesh was placed in. Meanwhile, the value of absorbance increased a lot when the mesh was changed from structure A to structure C. For quantitative analysis, the concentration of MB solution is calculated using Beer-Lambert law:

$$\lg(\frac{1}{T}) = \mathrm{K}bC \tag{1}$$

Where K is a constant, T, b and C are the transmittance, thickness and concentration of MB solution respectively. In our experiment, b and K are both constant, so Eq. (1) could be rewritten as

$$C = \frac{\lg(\frac{1}{T})}{\mathrm{K_b}} \tag{2}$$

Where $\mathrm{K_b}=\mathrm{K}b$. The calculated degeneration after irradiation of 450 s is shown for solution photocatalysed by structure A, B and C, respectively, in Fig. 5(b). The absorbance of light for water with corresponding mesh is also given. The PCD of MB solution is shown to increase proportionally with the increase of light absorbance. As a first order reaction, the relationship between concentration of MB solution and PCD reaction time could be described by

$$-\ln(\frac{C_t}{C_0}) = kt \tag{3}$$

Where C_0 is the original concentration of MB solution, t is reaction time, C_t is the concentration of MB solution at time t and k is a constant, which represents the of efficiency photocatalyst. Considering Eq. (3) and Fig. 5(b), the value of k is improved more than 60% by changing structure A to C, which means that the PCD reaction of MB solution could be modulated by design of photocatalyst structure.

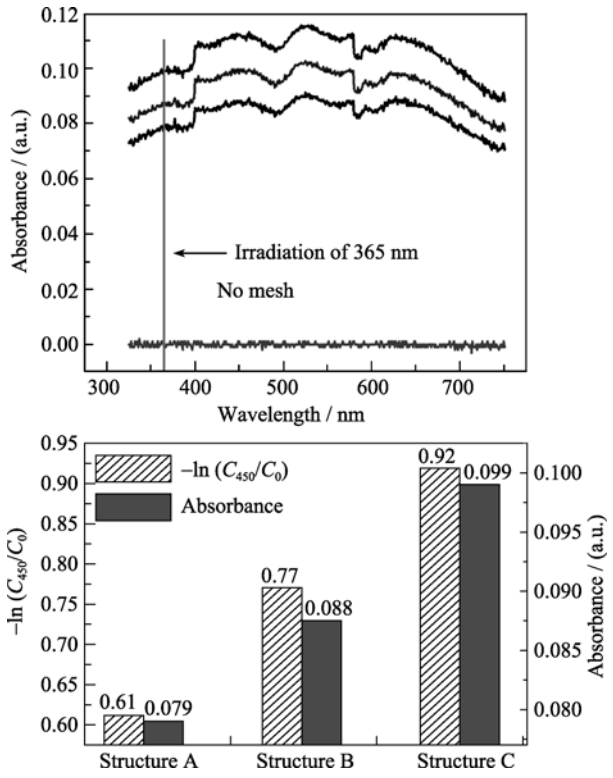

Fig. 5　(a) UV-Visible absorption spectra of 1.5 mL water, with meshes placed in, and (b) the calculated degeneration of MB solution photocatalysed by structure A, B and C, respectively, for irradiation of 450 s. Absorbance of light in water with the corresponding mesh under UV irradiation of 365 nm is also illustrated

It should be claimed that the PCD properties of titania suspension might be better than that of the direct-write structures, because of great specific surface area and strong adsorbility of nanoparticles. However, it is much easier to remove photocatalyst in the form of sintered mesh than in a dispersed form for the post-treatment of solutions. Meanwhile, the sintered mesh provides higher structure strength, better durability and space utilization, which is very helpful in water purification. So the effect of structure design on the PCD properties of photocatalyst was mainly concerned in this paper, without comparison to that of titania in a dispersed form or as a supported photocatalyst.

3　Conclusion

3D mesh structures has been constructed from a water based TiO_2 ink and sintered to rutile phase for PCD properties study. Three kinds of mesh structures have been designed and tested. Results show that reasonable design of mesh structure will cause significant enhancement in the PCD activity of photocatalyst. This enhancement could be explained by irradiation absorption increment, which is caused by structure design of photocatalyst. The sintered mesh structures can allow further breadth of application of TiO_2 into photocatalysis.

References:

[1] Serpone N, Pelizzetti E. Photocatalysis: Fundamentals and Applications. New York : Wiley, 1989: 619.

[2] Gaya U I, Abdullah A H. Heterogeneous photocatalytic degradation of organic contaminants over titanium dioxide: a review of fundamentals, progress and problems. *J. Photoch. Photobio. C*, 2008, **9(1):** 1–12.

[3] Park H, Choi W. Visible-light-sensitized production of hydrogen using perfluorosulfonate polymer-coated TiO_2 nanoparticles: an alternative approach to sensitizer anchoring. *Langmuir*, 2006, **22(6):** 2906–2911.

[4] Park H, Bae E, Lee J J, *et al*. Effect of the anchoring group in Ru-bipyridyl sensitizers on the photoelectrochemical behavior of dye-sensitized TiO_2 electrodes: carboxylate versus phosphonate linkages. *J. Phys. Chem. B*, 2006, **110(17):** 8740–8749.

[5] Lee J S, Choi W Y. Photocatalytic reactivity of surface platinized TiO_2: substrate specificity and the effect of Pt oxidation state. *J. Phys. Chem. B*, 2005, **109(15):** 7399–7406.

[6] Park H, Choi W. Photocatalytic reactivities of Nafion-coated TiO_2 for the degradation of charged organic compounds under UV or visible light. *J. Phys. Chem. B*, 2005, **109(23):** 11667–11674.

[7] Kim J, Choi W, Park H. Effects of TiO_2 surface fluorination on photocatalytic degradation of methylene blue and humic acid. *Res. Chem. Intermed.*, 2010, **36(2):** 127–140.

[8] Minero C, Mariella G, Maurino V, *et al*. Photocatalytic transformation of organic compounds in the presence of inorganic anions. 1. Hydroxyl-mediated and direct electron-transfer reactions of phenol on a titanium dioxide-fluoride system. *Langmuir*, 2000, **16(6):** 2632–2641.

[9] Cai K, Sun J, Wang R, *et al*. Direct-writing construction of layered meshes from nanoparticles-vaseline composite inks: rheological properties and structures. *Appl. Phys. A*, 2010, **102(2):** 501–507.

[10] Lu X S, Lee Y, Yang S F, *et al*. Solvent-based paste extrusion solid freeforming. *J. Eur. Ceram. Soc.*, 2010, **30(1):** 1–10.

[11] Lewis J A, Smay J E, Stuecker J, *et al*. Direct ink writing of three-dimensional ceramic structures. *J. Am. Ceram. Soc.*, 2006, **89(12):** 3599–3609.

[12] Smay J E, Cesarano J, Tuttle B A, *et al*. Directed colloidal assembly of linear and annular lead zirconate titanate arrays. *J. Am. Ceram. Soc.*, 2004, **87(2):** 293–295.

[13] Griffith L G, Naughton G. Tissue engineering - current challenges and expanding opportunities. *Science*, 2002, **295(5557):** 1009–1014.

[14] Gratson G M, santamaria F G, Lousse V, *et al*. Direct-write assembly of three-dimensional photonic crystals: conversion of polymer scaffolds to silicon hollow-woodpile structures. *Adv. Mater.*, 2006, **18(4):** 461–465.

[15] Garcia-Santamaria F, Xu M J, Lousse V, *et al*. A germanium inverse woodpile structure with a large photonic band gap. *Adv. Mater.*, 2007, **19(12):** 1567–1570.

[16] Gates B D. Flexible electronics. *Science*, 2009, **323(5921):** 1566–1567.

[17] Ahn B Y, Duoss E B, Motala M J, *et al*. Omnidirectional printing of flexible, stretchable, and spanning silver microelectrodes. *Science*, 2009, **323(5921):** 1590–1593.

[18] Yoneyama H, Tamura H, Toyoguch Y. Reduction of methylene-blue on illuminated titanium-dioxide in methanolic and aqueous-solutions. *J. Phys. Chem.*, 1972, **76(23):** 3460–3464.

[19] Chen R F, Zhang L, Wei Y, *et al*. Preparation of rutile (TiO_2) nanostructured materials at low temperature from $TiCl_4$ aqueous solution. *J. Mater. Sci.*, 2007, **42(17):** 7141–7146.

三维 TiO_2 陶瓷网络的直写无模成型及结构设计对其光催化性能的调制作用

蔡坤鹏[1,2], 李亚运[1], 孙振新[1], 孙竞博[1], 李 勃[1,2], 周 济[1]

(1. 清华大学 材料科学与工程系, 新型陶瓷与精细工艺国家重点实验室, 北京 100084; 2. 清华大学 深圳研究生院, 新材料研究所, 深圳 518055)

摘 要: 通过浆料直写无模成型技术制备了三维的 TiO_2 网络结构, 所得结构在空气中 1150℃的条件下煅烧 2 h, 并用于亚甲基蓝的光催化分解. 分别通过 X 射线衍射和扫描电子显微镜研究了烧成样品的物相结构和形貌. 用紫外–可见分光光度计表征了烧成样品的光催化分解性能, 结果显示本结构样品的光催化性能优于同质量的圆柱状样品. 此外, 本实验设计了三种不同的网络结构, 烧成后进行光催化降解性能测试. 结果显示: 通过合理的结构设计, 网络样品的光催化降解性能可提高大于 60%的程度. 样品催化性能的提高可归因于催化剂结构设计所带来的材料对光辐射吸收的增强.

关 键 词: 直写成型; 陶瓷; 光催化; TiO_2

中图分类号: TB321 **文献标识码:** A